Pergamon

Comput. Biol. Med. Vol. 27, No. 1, pp. 9–18, 1997
© 1997 Elsevier Science Ltd. All rights reserved
Printed in Great Britain
0010-4825/97 $17.00+0.00

PII: S0010-4825(96)00038-8

MULTI-UNIT SPIKE DISCRIMINATION USING WAVELET TRANSFORMS

GEORGE ZOURIDAKIS[a]* and DAVID C. TAM[b]

[a] Department of Neurosurgery, University of Texas-Houston Medical School, 6431 Fannin, Suite 7.148, Houston, TX 77030, U.S.A.

[b] Department of Biological Sciences, Center for Network Neuroscience, University of North Texas, TX 76203, U.S.A.

(*Received* 29 *August* 1995; *revised* 19 *September* 1996)

Abstract—A new spike discrimination procedure addressing the specific problem of spike superposition is described. The method, based on a shift-invariant wavelet transform and its amplitude-and-phase representation, has the advantage of both reducing the effect of noise present in the data and correcting the latency of specific components in a waveform. When spikes overlap and produce unknown patterns, the procedure extracts the constituent spikes and also estimates their exact time of occurrence. Fast implementation algorithms, having complexity of at most $\mathcal{O}(N \log N)$, allow the use of the method in real-time applications. © 1997 Elsevier Science Ltd

Multi-unit spike train Spike discrimination Wavelet transform Shift-invariant transform

1. INTRODUCTION

Electrical signals generated by neurons, referred to as *action potentials* or *spikes*, can be recorded extracellularly by an adjacent electrode, which may detect the activity of several neurons firing simultaneously. However, the waveforms produced on the extracellular electrode are often distinct and, therefore, individual cells can be identified by analyzing their characteristic patterns of activity. In this way, it is possible to separate a multi-unit recording into several spike trains, each containing the activity of one cell only.

Spike discrimination can be accomplished easily using conventional waveform analysis techniques, such as template matching, if the signal-to-noise ratio is sufficiently high and the spikes generated by different neurons do not overlap. The spike-separation procedure becomes nontrivial when there is partial or complete overlap of spikes originating from several neurons.

During the past several years, a large number of spike-discrimination methods have been developed, including single- and multi-channel template matching [1–5], principal-component analysis [6], amplitude separation [7], Fourier analysis [8], linear filtering [9], velocity analysis [10], autoregressive modeling [11], neural networks [12], and maximum likelihood approaches [13,14]. Some of these methods have been reviewed by Schmidt [15,16].

The difficulty in resolving overlapping spikes, encountered by most discrimination procedures, is primarily due to the fact that neurons do not necessarily fire exactly at the same time, but there may be some delay between the firing of, say, two neurons. This delay is small enough to cause spikes to overlap and, at the same time, it is long enough to cause the peaks of the spikes to be misaligned. This delay, and differences in the shape and size of individual spikes, result in new, unpredictable patterns on the recording electrode. The spike-extraction algorithm should be able to distinguish such patterns from nonoverlapping ones and separate them into their constituent spikes.

Most of the existing methods perform very well when the problem of overlapping spikes

* Author to whom correspondence should be addressed.

is not considered. However, methods that do not deal with such an important issue potentially may ignore critical information about synchronized activity in a network of neurons. Other limitations of the existing techniques concern their degree of success in the case of multiple templates, their ease of hardware and/or software implementation, their portability across platforms, and their suitability for real-time processing.

We have proposed a new method for multi-unit spike discrimination that addresses some specific problems associated with spike overlaps [17]. The method is based on a shift-invariant wavelet transformation and a particular representation of the "magnitude" and "phase" of the transformed signals. As will be explained later, this representation has the advantage of both reducing the effect of noise present in the data and of correcting the latency of specific components in a waveform.

The whole discrimination procedure consists of two steps: a *learning stage*, during which the number of neurons contributing to a particular recording is estimated and appropriate spike templates are created; and a *classification stage*, during which the exact time of occurrence and the neuron of origin are computed for each spike in the trace.

The learning stage uses a small portion of the data[1] to create reliable templates [18] and is based on a well-known fuzzy clustering procedure (e.g. see [19]). This approach yields more reliable templates than the conventional procedures [20], since fuzzy methods are better suited to deal with incomplete and/or ambiguous information [21]. In this article we report the methods used during the classification stage only. The same method can be employed to study characteristic components of other electrophysiological signals, such as epileptogenic spikes in the EEG.

2. METHODS

2.1. *Fast discrete wavelet transform*

The proposed method is based on the wavelet transform (WT). Rigorous mathematical treatise on WTs can be found, for instance, in [22] and [23]. Here we describe the basic ideas used by our procedure.

The *continuous WT* of a square-integrable function $f(t)$ is defined as

$$Wf(s,t)=\int_{-\infty}^{+\infty} f(\tau)\frac{1}{\sqrt{s}}\psi\left(\frac{t-\tau}{s}\right)d\tau, \tag{1}$$

where s and t are the scale (or frequency) and time variables, respectively. The function $\psi(t)$, called a *wavelet*, must satisfy the admissibility condition [23], i.e. it must be a zero-mean, square-integrable function. In practical applications the parameters s and t must be discretized. For instance, for a certain class of wavelets, s can be sampled along a *dyadic* sequence only, defined by

$$s=2^j, \text{ with } j\in\mathfrak{Z}, \tag{2}$$

without modifying the overall properties of the transform. Then, the *dyadic WT* of a discrete signal $f(n)$ can be obtained through an iterative procedure proposed by Mallat [24], which, at each scale 2^j, decomposes $f(n)$ into a "lower resolution" signal $S_{2^{j+1}}f$ and an "added detail" signal $W_{2^{j+1}}f$, through lowpass and bandpass filtering, as follows,

$$S_{2^{j+1}}f(n)=S_{2^j}f(n) * h_j(n), \tag{3}$$

$$W_{2^{j+1}}f(n)=S_{2^j}f(n) * g_j(n). \tag{4}$$

The discrete functions $h(n)$ and $g(n)$ correspond to the lowpass and bandpass filters, respectively. The algorithm has an asymptotic complexity of at most $\mathcal{O}(N \log N)$ depending on the number of nonzero coefficients of $h(n)$ and $g(n)$. The functions $h_j(n)$ and $g_j(n)$ are obtained by inserting 2^j-1 zeros between the coefficients of the filters $h(n)$ and $g(n)$

[1] Alternatively, templates could be updated during classification, too.

(corresponding to dilated filters with transfer functions $H(2^j\omega)$ and $G(2^j\omega)$, respectively).

The original function $f(n)$ can be reconstructed from its dyadic WT through a similar iterative procedure, which, at each scale 2^j reconstructs $S_{2^{j-1}}f$ from $S_{2^j}f$ and $W_{2^j}f$,

$$S_{2^{j-1}}f(n)=W_{2^j}f(n) * \tilde{g}_{j-1}(n)+S_{2^j}f(n) * \tilde{h}_{j-1}(n). \tag{5}$$

The functions $\tilde{H}$ and $\tilde{g}$ denote filters whose transfer functions $\tilde{H}(\omega)$ and $\tilde{G}(\omega)$ are the complex conjugates of $H(\omega)$ and $G(\omega)$, respectively. In particular, $\tilde{g}(n)=g(-n)$. The complexity of the reconstruction algorithm is also $\mathcal{O}(N \log N)$. To take care of "edge-effect" problems, the signal $f(n)$ is "periodized" before filtering.

2.2. *Shift-invariant representation*

Given a function $f(n)$ and its (discrete dyadic) wavelet transform

$$WTf=\{Sf_{2^J}(n);\{Wf_{2^j}(n)\}_{j\in[1,J]},J\in\mathcal{Z}\}, \tag{6}$$

it is possible to create two new vectors representing the "magnitude" and "phase" of WTf. The *magnitude* vector $\mathcal{M}(WTf)$ is obtained by simply sorting the values of the vector $\{Wf_{2^j}(n)\}_{j\in[1,J]}$ in increasing order. The *phase* vector $\mathcal{P}(WTf)$ is obtained by indicating the position that each component of the magnitude vector had in the original WTf prior to sorting. The two new vectors define a complete and stable transform, i.e. it is always possible to reconstruct the original WTf, and therefore $f(n)$, from this *amplitude-and-phase* pair. The advantage of this new representation is that it is *phase (shift) invariant*. That is, a transient signal $x(n)$ and all of its time-shifted versions $x_{n_0}(n)=x(n-n_0)$ with $n_0\in\mathcal{Z}$ have identical magnitudes, i.e. $\mathcal{M}(WTx_{n_0})=\mathcal{M}(WTx)$ for all $n_0\in\mathcal{Z}$. The phase vectors $\mathcal{P}(WTx_{n_0})$ and $\mathcal{P}(WTx)$, however, may be different.

2.3. *Phase correction algorithm*

Assuming that an original signal (template) $x(n)$ is known—thus the vectors $\mathcal{M}(WTx)$ and $\mathcal{P}(WTx)$ are also available—it is possible to correct the phase of an arbitrarily shifted sequence $x_{n_0}(n)$ through the following steps.

1. Compute WTx_{n_0}, the WT of the shifted sequence $x_{n_0}(n)$.
2. Construct the magnitude and phase pair, $\mathcal{M}(WTx_{n_0})$ and $\mathcal{P}(WTx_{n_0})$, respectively.
3. Replace the phase vector $\mathcal{P}(WTx_{n_0})$ of the shifted sequence with the phase vector $\mathcal{P}(WTx)$ of the template.
4. Compute the inverse transform of the resulting magnitude-and-phase pair $\{\mathcal{M}(WTx_{n_0}), \mathcal{P}(WTx)\}$ to obtain a reconstructed signal $x^*(n)$.

The last signal $x^*(n)$ is a phase-corrected approximation of the original template $x(n)$ and, under the ideal condition of absence of noise, these two signals will be (almost) identical. The exact amount n_0 of time-shift between $x(n)$ and $x_{n_0}(n)$ is given by the following expression,

$$\left| \max_i \mathcal{P}(WTx) - \max_i \mathcal{P}(WTx_{n_0}) \right|,$$

where $\max_i \mathcal{P}(\cdot)$ indicates the component corresponding to the maximum index of the phase vector.

2.4. *Graphical illustration of the method*

The following paragraphs give a graphical illustration of the methods described earlier. In our computations we used the lowpass and bandpass filters ($h(n)$ and $g(n)$, respectively) reported by Mallat [24] and Mallat and Zhong [25]. Figures 1a and 1c show these filters in the time domain and Fig. 1b and 1d depict their transfer functions, $H(\omega)$ and $G(\omega)$, respectively. The frequency axes are normalized to the sampling rate. The latter figures show that $h(n)$ and $g(n)$ indeed correspond to a lowpass and a bandpass filter, respectively.

Figure 2 illustrates the use of the iterative algorithms defined in equations (3) and (4) to compute the wavelet transform of a signal. The original sequence in this example is a typical spike (consisting of 128 samples) recorded extracellularly from a crayfish neuron (see Fig. 2a). The signals obtained after successive application of the lowpass and bandpass filters (resulting in the so-called *multiresolution decomposition*) are shown in Fig. 2b and 2c, respectively. The corresponding wavelet transform is shown in Fig. 2d.

The process of decomposing the wavelet transform of the original signal into its magnitude and phase representation is shown schematically in Fig. 3. Figure 3a shows the original signal, Fig. 3b its wavelet transform, and Fig. 3c the corresponding magnitude-and-phase representation.

3. APPLICATION EXAMPLES

3.1. *Phase correction of test signals*

Figure 4 illustrates the procedures to perform phase correction on a time-shifted signal using the shift-invariant wavelet transform and its magnitude-and-phase representation. The original signal and a time-shifted version of it are shown in Fig. 4a (left and right column, respectively). Figure 4b depicts the corresponding magnitude-and-phase representations. Note that the magnitude vectors are identical, but the corresponding phase vectors are different. The phase of the time-shifted signal can be corrected in the wavelet domain by replacing the phase vector of the shifted signal with the phase vector of the template (the original signal). By taking the inverse wavelet transform of the resulting signal, the phase of the time-shifted signal is restored to that of the original unshifted one. Figure 4c shows that the original and the reconstructed signals are practically identical.

To show the further advantage of noise reduction resulting from the shift-invariant

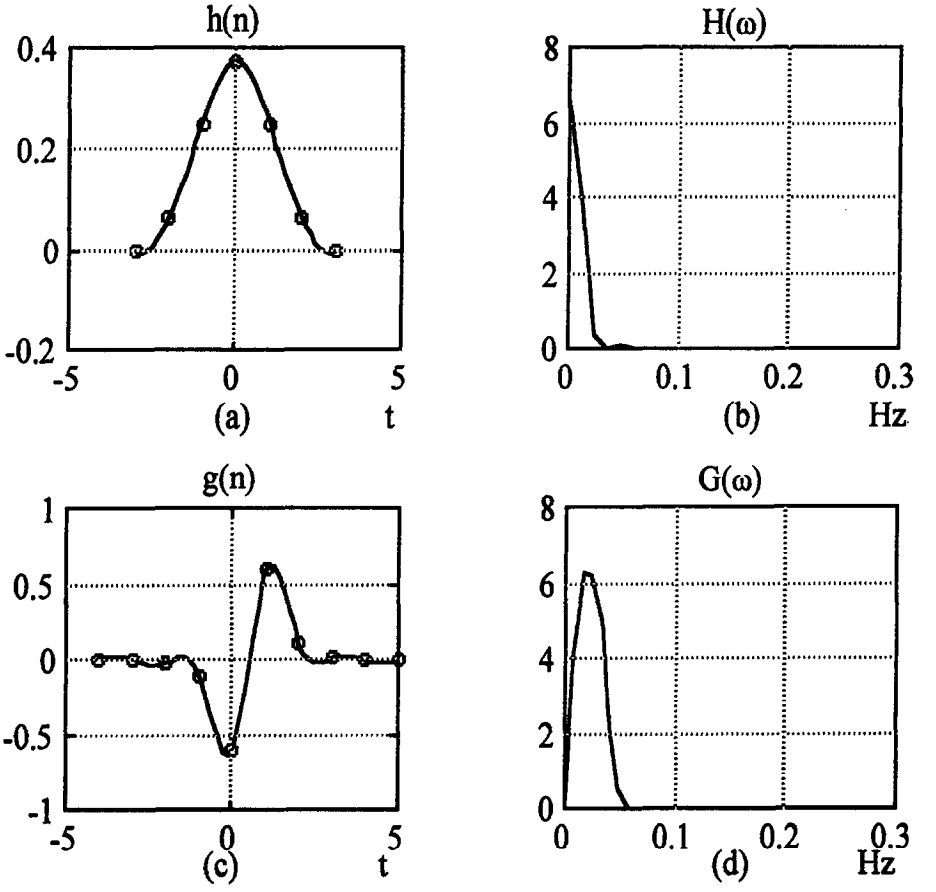


Fig. 1. Lowpass $h(n)$ and bandpass $g(n)$ filters used to compute discrete wavelet transforms, and the corresponding transfer functions, $H(\omega)$ and $G(\omega)$.

transformation, we consider the transformation of some noisy test signals. Figure 5 illustrates the same procedure for a square wave and a spike (left and right column of Fig. 5a, respectively). In addition to time-shifting the original signals, some (zero mean, Gaussian) noise was added to their amplitudes (Fig. 5b). As can be seen in Fig. 5c, the inverse transformation not only corrected the phase of the transients, but also reduced the effect of the additive noise on the reconstructed signals.

3.2. *Spike-train analysis*

The method described previously was applied to the specific problem of spike detection and classification, whereby the ability of the algorithm to resolve overlapping spikes is critical. To ensure that we could identify spikes without ambiguity, we created a spike train in which the shape and location of the spikes were known, and some of the spikes were overlapping in time. Furthermore, we corrupted the resulting signal with additive noise. Then, we applied our classification algorithm to identify the exact time location and the neuron of origin of each spike.

The synthetic spike train was generated as follows. First, a short segment of data recorded from crayfish neurons was used to extract characteristic spikes (templates) representing the activity of two distinct neurons. The same data set was also used to obtain "silent" periods, i.e. portions of the recording that contained background activity (noise) only. Then, two spike trains (one for each neuron) were constructed by obtaining the time of occurrence of spikes from a random sequence with Poisson distribution representing interspike intervals. To simulate noise disturbances in the spike profiles of both templates, the spike amplitudes were multiplied by a random number (uniformly distributed between

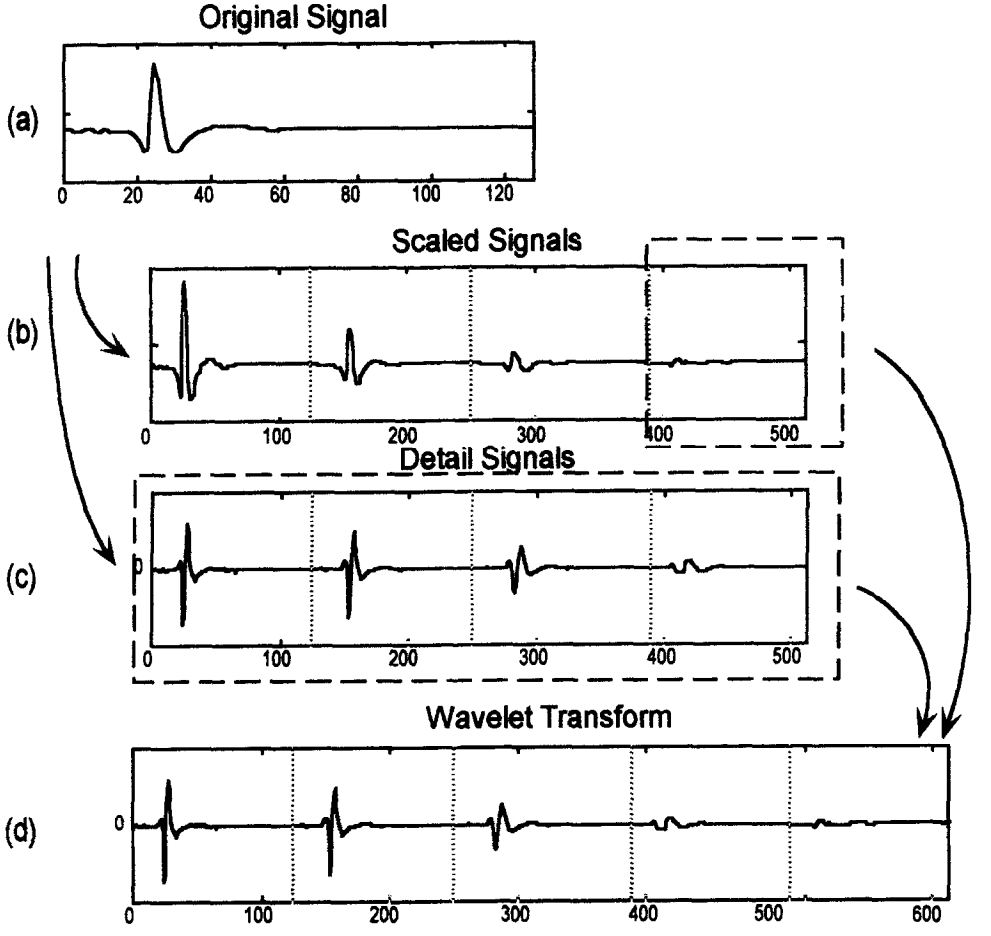


Fig. 2. Examples of multiresolution decomposition and resulting wavelet transform of a transient signal.

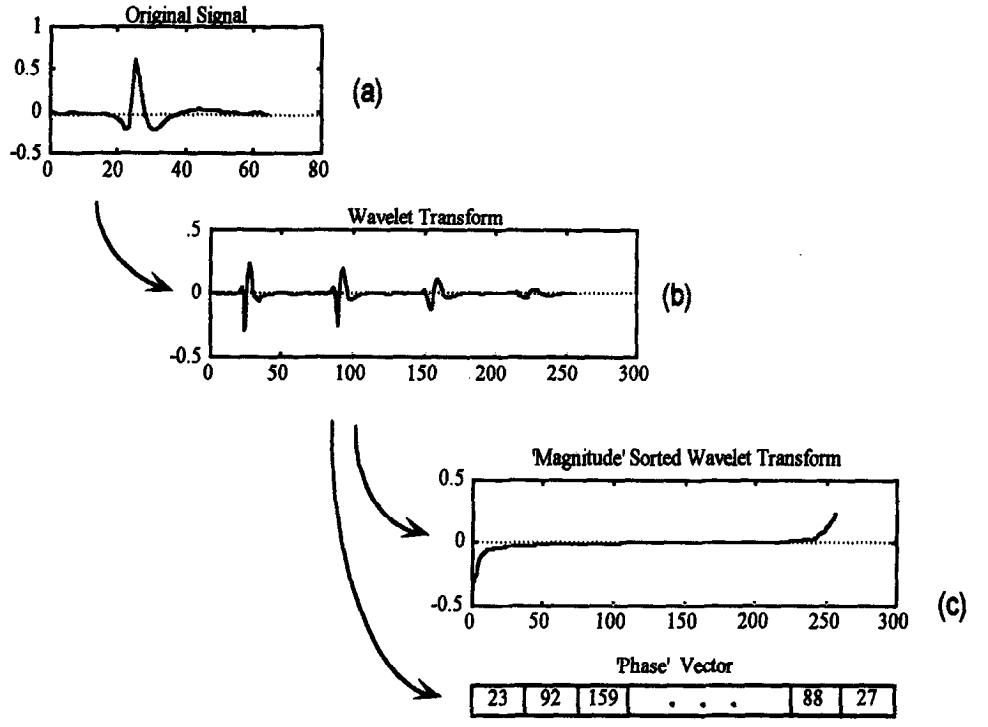


Fig. 3. Example of magnitude and phase representation of a test signal.

0.9 and 1.1) prior to their insertion into the spike trains. The two independent spike trains were then merged into one to simulate the simultaneous activity of both neurons recorded from a single electrode. Since the location of individual spikes was randomly determined, some of the spikes could also overlap in time (partially or totally). Finally, the noise segments (after being normalized to zero mean and known variance σ) were added to the synthetic spike train. A portion of the resulting time series is shown in Fig. 6.

This synthetic spike train was presented to the classifier which first detected each spike and then classified it into one of two known classes, termed **class 1**, and **class 2**, respectively. When activity was identified as the result of overlapping spikes, the class of each of the constituent spikes and the amount of overlap was determined. An **unknown**

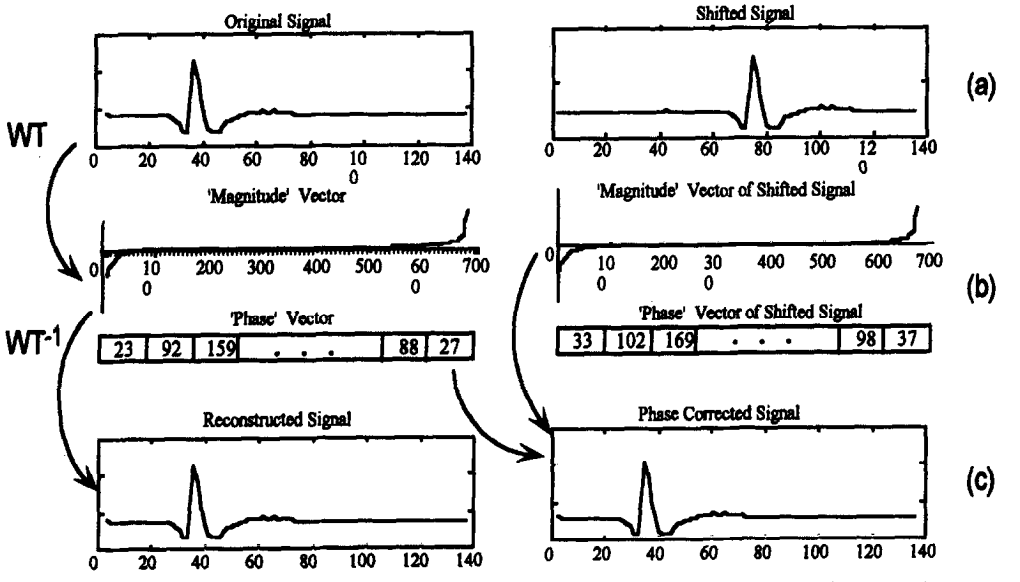


Fig. 4. Examples of latency correction of transient signals using the shift-invariant wavelet transform.

class was also possible, for the cases whereby the algorithm could not assign the spike to any of the known classes. Table 1 shows the latencies of the spikes that the algorithm was able to detect. In this case, three overlaps were identified. Figure 7 shows an example of overlapping spikes which the algorithm was able to detected and correct their phases. The overall performance of the classifier for this data segment is summarized in Table 2.

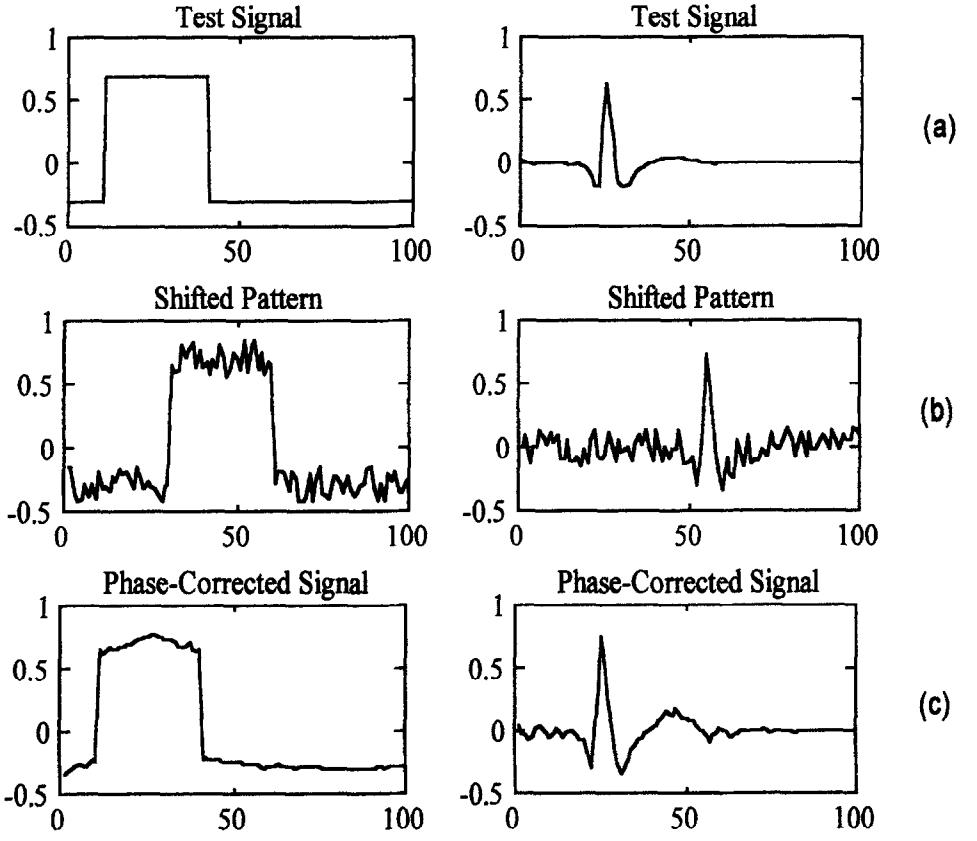


Fig. 5. Examples of phase correction/noise reduction of noisy transients using the shift-invariant wavelet transform.

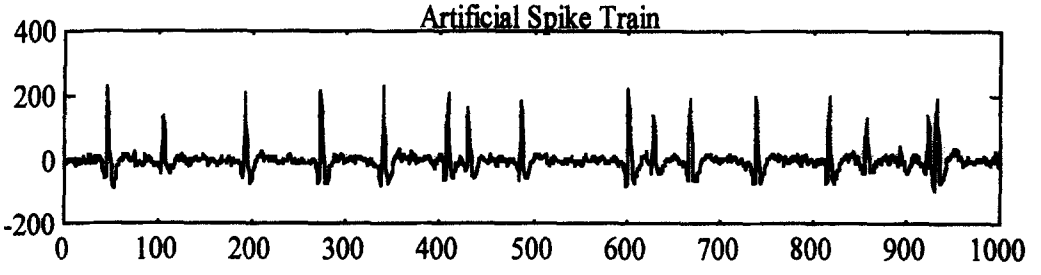


Fig. 6. Example of a spike train generated to test the shift-invariant wavelet transform classification procedure.

Table 1. Latency of the spikes detected by the discrimination algorithm for **class 1** and **class 2**

Class	Latency										
Class 1	46	192	273	339	408	487	602	668	739	817	932
Class 2	105	430	629	857	923						
Both	408	602	923								

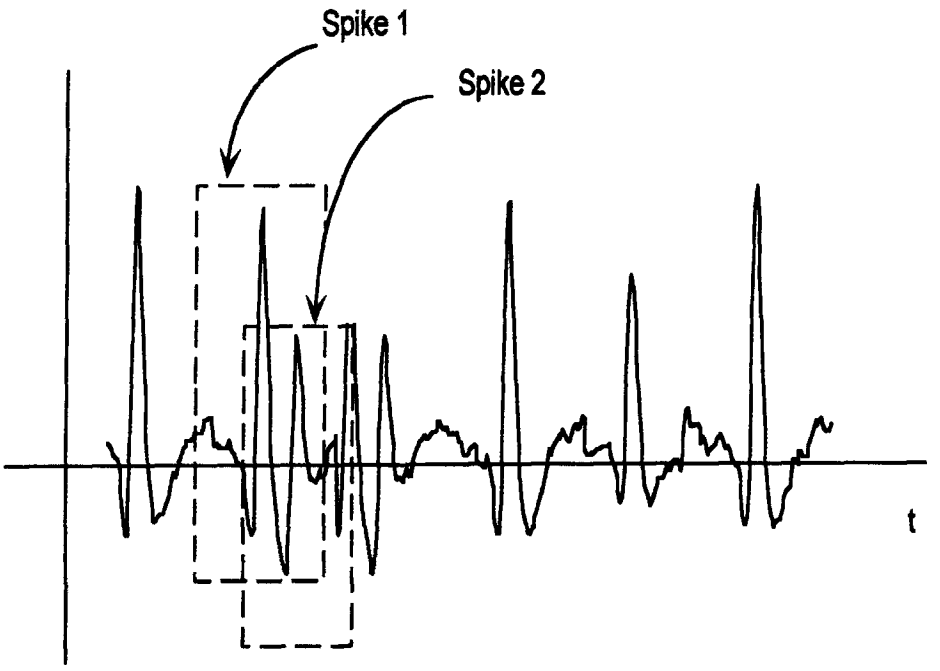


Fig. 7. Example of overlapping spikes detected by the classification algorithm.

4. CONCLUSIONS

A new method has been presented to address the specific problem of spike superposition, which is a limitation in most multi-unit spike discrimination procedures found in the literature. In fact, overlapping spikes occur frequently in single electrode recordings when neurons fire synchronously. When the spike-detection algorithm ignores the issue of spike superposition, these events will be missed, and as a result, the synchronization of firing in neurons will be underestimated. The latter may represent a significant consequence of correlated activity in neural networks.

The method described in this paper is part of a larger spike discrimination procedure, which can identify the exact time of occurrence and the neuron of origin for all spikes in a recording. In cases where spikes overlap to produce some new pattern, the algorithm extracts the constituent spikes and estimates their time of occurrence by performing phase correction on individual spikes. Our approach is based on a shift-invariant wavelet transform and a particular magnitude-and-phase representation of the transformed signals. The advantage of such a representation is twofold: it reduces the effect of noise present in the data, and also, it corrects the phase (latency) of specific components in a waveform.

The performance of our procedure depends on the availability of "good" spike templates, which are difficult to obtain in real time applications, because the initial data segment usually used as a "learning set" does not account for the variability of the spikes in the whole data. However, our spike templates are obtained using a fuzzy clustering approach, which was proven to give better results than the conventional procedures [20].

Table 2. Performance table on data with $\sigma=10$. Rows represent the actual class of a spike and columns the classification result

	class 1	class 2	Correct
Class 1	11	0	11
Class 2	0	5	5
Both	3	3	6
Total	14	8	22

The above examples illustrate the technique on simulated data (synthetic spike trains), and also demonstrate that this procedure can be applied successfully to real recordings. The discrete wavelet transform can be implemented through a very fast algorithm, whose complexity is at most $\mathcal{O}(N \log N)$, thus making it very appealing for on-line applications. Detailed information on fast WTs, implementation of fast algorithms, and specific applications can be found, for example, in [26–28].

The use of the proposed method is not limited to spike-train analysis only, but it can be applied to other fields of waveform recognition such as EEG and evoked potentials.

5. SUMMARY

A new multi-unit spike-discrimination procedure has been presented to address the specific problem of spike superposition. Overlapping spikes, originating from several neurons, occur frequently in single electrode recordings, resulting in new unpredictable patterns. Detection of spike superpositions can give significant information as regards synchronization of activity in a biological neuronal network. Thus, the spike-extraction algorithm should be able to distinguish such patterns and separate them into their constituent spikes.

Our procedure is based on a shift-invariant wavelet transform and its amplitude-and-phase representation. It has the advantage of both reducing the effect of noise present in the data and correcting the latency of specific components in a waveform. The algorithm can identify the time of occurrence and the neuron of origin for all spikes in a recording. When spikes overlap and produce unknown patterns, the algorithm extracts the constituent spikes and also estimates their exact time of occurrence.

Extensive simulations with synthetic spike train (generated from segments of data recorded from crayfish neurons containing spikes and "silent" periods of background noise) demonstrate that this procedure can be applied successfully to real recordings as well. Fast implementations of the algorithm, having complexity of at most $\mathcal{O}(N \log N)$, allow its use in real-time applications. The same method can also be employed to study characteristic components of other electrophysiological signals, such as epileptogenic spikes in the EEG.

Acknowledgements—This research was supported in part by Office of Naval Research Grant numbers N00014-94-1-0686 and N00014-93-1-0135 to DCT.

REFERENCES

1. E. d'Hollander and G.A. Orban, Spike recognition and on-line classification by unsupervised learning system, *IEEE Trans. Biomed. Eng.*, **26**, 279–284 (1979).
2. G.J. Dinning and A.C. Sanderson, Real-time classification of multi-unit neural signals using reduced feature sets, *IEEE Trans. Biomed. Eng.*, **28**, 804–811 (1981).
3. R. Millecchia and T. McIntyre, Automatic nerve impulse identification and separation, *Comput. Biomed. Res.*, **11**, 459–468 (1978).
4. M. Salganicoff, M.F. Saxna, L. Sax and G.L. Gertein, Unsupervised waveform classification for multineuron recordings: a real-time, software based system I. Algorithms and implemetation, *J. Neurosci. Meth.* , **25**, 181–488 (1988).
5. J.F. Vibert, J.N. Albert and J. Costa, Intelligent software for spike separation in multiunit recordings, *Med. Biol. Eng. Comput.*, **25**, 366–372 (1987).
6. M. Abeles and M.H. Goldstein, Multispike train analysis, *IEEE Trans. Biomed. Eng.*, **65**, 762–773 (1977).
7. H. Bergman and M.R. DeLong, A personal computer-based spike detector and sorter: implementation and evaluation, *J. Neurosci. Meth.* , **41**, 187–197 (1992).
8. K.C. MeGill and L.J. Doffman, High-resolution alignment of sampled waveforms, *IEEE Trans. Biomed. Eng.*, **31**, 462–468 (1984).
9. W.M. Roberts and D.K. Hartline, Separation of multiunit nerve impulse trains by a multichannel linear filter algorithm, *Brain Res.* , **94**, 141–149 (1975).
10. M. Brunner, G. Karg and U.T. Koch, An improved system for single unit isolation from multiunit nerve recordings by velocity analysis, *J. Neurosci. Meth.* , **33**, 1–9 (1990).
11. L. Liu, A method of neuronal spike train study based on autoregressive analysis, *Biol. Cybern.*, **61**, 289–293 (1989).
12. R.F. Jansen, The reconstruction of individual spike trajns from extracellular multi-unit recordings using a neural network emulation program, *J. Neurosci. Meth.* , **35**, 203–213 (1990).
13. A.F. Atiya, Recognition of multiunit neural signals, *IEEE Trans. Biomed. Eng.*, **39**, 723–729 (1992).
14. D.R. Brillinger and R. Miller, The maximum likelihood approach to the identification of neuronal firing systems, *Ann. Biomed. Eng.*, **16**, 3–16 (1988).

15. E.M. Schmidt, Computer separation of multi-unit neuroelectric data: a review, *J. Neurosci. Meth.* , **12**, 95–111 (1984).
16. E.M. Schmidt, Instruments for sorting neuroelectric data: a review, *J. Neurosci. Meth.* , **12**, 1–24 (1984).
17. G. Zouridakis and D.C. Tam, The use of wavelet transforms in multi-unit spike discrimination. 22nd Annual Meeting, Society for Neuroscience, Anaheim, CA (1992)
18. G. Zouridakis and D.C. Tam, Identification of spike profiles using fuzzy-logic classifiers. 23rd Annual Meeting, Society for Neuroscience, Washington DC (1993).
19. L. Kaufman, *Finding Groups in Data: An Introduction to Cluster Analysis*, L. Kaufman and P. J. Rousseuw (Eds). Wiley, New York (1989).
20. G. Zouridakis and D.C. Tam, Recognition and classification of multineuron activity using a fuzzy-clustering approach. In *Computational Medicine, Public Health, and Biotechnology: Building a Man in the Machine.* World Scientific, New York (1995).
21. G. Zouridakis, B.H. Jansen and N.N. Boutros, A fuzzy clustering approach to EP estimation, *IEEE Trans. Biomed. Eng.*, in press.
22. A. Grossmann and J. Motlet, Decomposition of Hardy functions into square integrable wavelets of constant shape, *SIAM J. Math.*, **15**, 723–736 (1984).
23. I. Daubechies, Ten lectures on wavelets. *CBMS-NSF Series Appl. SIAM Math.* (1992).
24. S. Mallat, Zero-crossing of a wavelet transform, *IEEE Trans. Inform. Theory*, **37**, 1019–1033 (1991).
25. S. Mallat and S. Zhong, Characterization of signals from multiscale edges, *IEEE Trans. Pattern Anal. Machine Intell.* , **14**, 710–732 (1992).
26. G. Belkin, Fast wavelet transforms and fast algorithms. In Y. Meyer (Ed.), *Wavelets and Applications*, pp. 254–367. Masson, Paris (1992).
27. M.A. Cody, The fast wavelet transform. *Dr. Dobb's Journal* April (1992).
28. M. Vetterli and J. Kovacevic, *Wavelets and Subband Coding*. Prentice Hall, Englewood Cliffs (1995).

About the Author—GEORGE ZOURIDAKIS was born in Chania, Greece, in 1962. He received the Dr. Ing. degree in Electronics Engineering from the University of Rome "La Sapienza" in Italy. In 1990 he received an MSc in Biomedical Engineering and in 1994 a PhD in Electrical Engineering both from the University of Houston. Currently he is an Assistant Professor in the Department of Neurosurgery, University of Texas Houston Medical School. His research interests include the development of techniques for pattern recognition and automated detection, quantification, and modeling of biosignals, especially with regard to electroencephalograms and evoked potentials. Emphasis is given in the area of nonlinear dynamics, fuzzy decision making, and wavelet transforms, with specific applications in neurology and psychiatry.

About the Author—DAVID C. TAM is currently an assistant professor in the Department of Biological Sciences and the Center for Network Neuroscience at the University of North Texas in Denton. He received three BSc degrees in Computer Science, Physics and Astrophysics in 1980 and 1984, and a PhD degree in Physiology in 1987, all from the University of Minnesota in Minneapolis. He was a research assistant professor in the Division of Neuroscience at Baylor College of Medicine in Houston from 1989 to 1992 engaged in research on computational neuroscience. He was a post-doctoral fellow at the Theoretical Neurobiology Facility at the University of California at Irvine from 1987 to 1989. His research interests include computational neuroscience, neural signal analysis, neural signal processing, neural modeling and neural network simulation as well as experimental multi-channel, multi-unit recording of neuronal electrophysiological signals from *in vitro* preparations of networks of cultured neurons and also from *in vivo* preparations.